ACS BIO & MED CHEM Au
AN OPEN ACCESS JOURNAL OF THE AMERICAN CHEMICAL SOCIETY

pubs.acs.org/biomedchemau
Article

High-Fidelity Assay Based on Turn-Off Fluorescence to Detect the Perturbations of Cellular Proteostasis

Conner Hoelzel,[⊥] Yulong Bai,[⊥] Mengdie Wang, Yu Liu,* and Xin Zhang*

Cite This: *ACS Bio Med Chem Au* 2024, 4, 111−118
Read Online

ACCESS | Metrics & More | Article Recommendations | Supporting Information

ABSTRACT: The persistence of neurodegenerative diseases has necessitated the development of new strategies to monitor protein homeostasis (proteostasis). Previous efforts in our laboratory have focused on the development of fluorogenic strategies to observe the onset and progression of proteostatic stress. These works utilized solvatochromic and viscosity sensitive fluorophores to sense protein folded states, enabling stressor screening with an increase in the emission intensity upon aggregation. In this work, we present a novel, high-fidelity assay to detect perturbations of cellular proteostasis, where the fluorescence intensity decreases with the onset of proteostatic stress. Utilizing a fluorogenic, hydroxymethyl silicon-rhodamine probe to differentiate between protein folded states, we establish the validity of this technology in living cells by demonstrating a two-fold difference in fluorescence intensity between unstressed and stressed conditions.

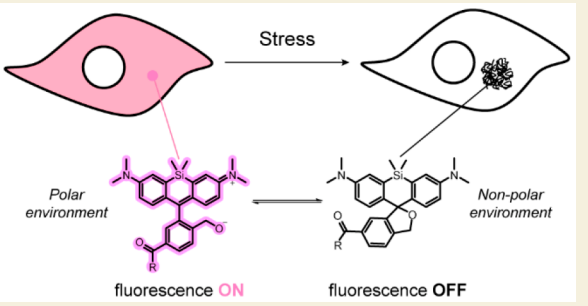

KEYWORDS: *rhodamine, fluorescence, aggregation, proteostasis, protein folding*

Various exogenous and cellular stress leads to protein misfolding that results in misfolded monomers, which proceed to form higher-order and cytotoxic soluble oligomers. This intermediate species preferably interact aberrantly with membranes, soluble proteins, or other cellular components to perturb native functions.[1−4] Finally, the progression of the intermediate oligomers to insoluble fibrils and aggregates hardly functions to attenuate the progression of the disease, as insoluble fibrils can act as a source for the generation of protein oligomers through secondary nucleation and further enable propagation from cell to cell.[5] The deposition of proteinaceous aggregates is associated with the progression of neurodegenerative diseases such as Alzheimer's, Parkinson's, and Huntington's diseases. A common trait of neurodegenerative diseases is the deleterious loss of function in subcellular organelles and structures, as the formation of irreversible protein aggregates sequesters the expressed protein, preventing the execution of the native physiological role. For instance, in Alzheimer's Disease, the depolymerization of microtubules is associated with the formation of neurofibrillary tangles of the microtubule binding protein, tau.[6] In other disorders, mitochondrial dysfunction and endoplasmic reticulum (ER) stress are observed as a result of aberrant interactions between protein aggregates and membranous structures.[7−9]

To visualize perturbations to the homeostasis of the proteome (proteostasis), many methods have been established in recent years.[10−13] Among them, our lab has developed AgHalo and AggTag technologies,[14−20] which rely on the utility of solvatochromic[14,20] and molecular-rotor based fluorophores[15−17] to differentiate between changes in the polarity and viscosity of the local microenvironment.[21−23] In these applications, the rigidity and hydrophobicity of misfolded oligomeric and aggregate species yield an increase in fluorescence intensity relative to the soluble, native conformation of the protein-probe conjugate. Together the AggTag and AgHalo systems are effective methodologies to visualize the onset of proteomic stress (Figure 1a). We aim to develop a high-fidelity, attenuation-of-signal method to detect the cellular proteostasis wherein the probe-protein conjugate brightly fluorescent in the folded conformation and nonemissive upon misfolding and aggregation.

Our designed method relies on the application of a small molecule probe that exhibits environmental sensitivity inverse to that of canonical solvatochromic probes. The application of such probes to the existing AgHalo and AggTag systems should enable visualization of the healthy, unstressed proteome as the fluorophore brightly fluorescent when localized to the polar, protic interface of the aqueous cytosol and protein surface. However, with stress-induced misfolding and aggregation of the protein-probe conjugate, the fluorophore will be localized to the hydrophobic, desolvated aggregate interior, yielding a decrease in emission intensity (Figure 1b). Through extensive review of

Received: February 5, 2023
Revised: January 3, 2024
Accepted: January 4, 2024
Published: January 19, 2024

https://doi.org/10.1021/acsbiomedchemau.3c00012
ACS Bio Med Chem Au 2024, 4, 111−118

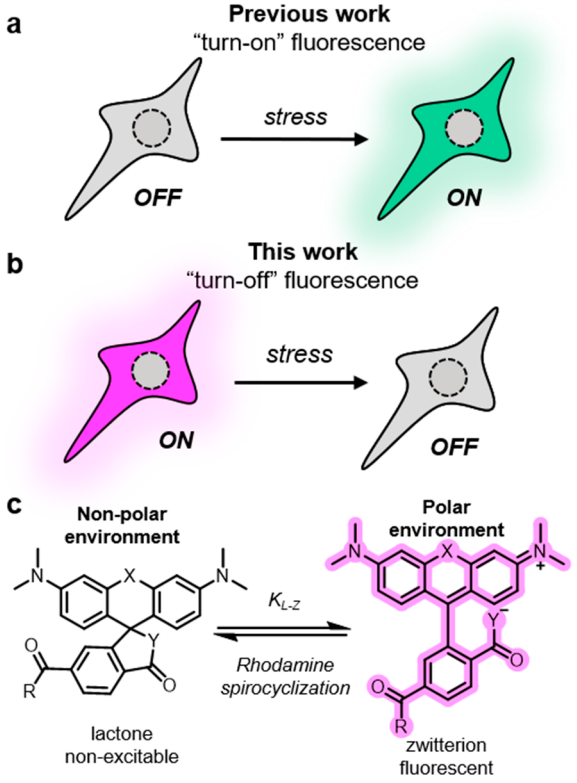

Figure 1. Methods of detecting perturbations to the homeostasis of the proteome. (a) Previous "turn-on" fluorescence assay. In the presence of a healthy, unstressed proteome, no fluorescence emission is observed (OFF). Stress induced protein misfolding and aggregation yields bright fluorescence emission (ON). (b) "Turn-off" fluorescence assay in this work. In the presence of a healthy, unstressed proteome, bright emission is observed (ON). Stress induced protein misfolding and aggregation yields a decrease in fluorescence emission (OFF). (c) Rhodamine environmental sensitivity originates from the polarity dependent equilibrium between the nonexcitable spirocyclic and fluorescent zwitterionic states.

literature, we have identified a candidate fluorophore system: fluorogenic rhodamine derivatives. Its environmental sensitivity results from a ground state spirocyclization process. This process is an inherent, polarity-dependent equilibrium between the emissive, zwitterionic conformer and the closed, nonexcitable spirocyclic form (KL-Z) (Figure 1c).[24−28] In nonpolar environments, KL-Z largely favors the spirocyclic conformer. Here, we investigate the application of rhodamine systems toward the aim of developing a proteostasis detecting assay.

The results detailed here establish the effective sensitization of the protein folded states utilizing the rhodamine platforms. Employing the existing metastable AgHalo protein system, we demonstrate that superior fold-change in emission intensity can be achieved via the structural tunability of rhodamine spirocyclization. The analysis of this sensitization *in vitro* enables the visualization of proteostasis in living cells with a hydroxymethyl silicon rhodamine derivative. Furthermore, our investigations indicate that this technology can be extrapolated from the AgHalo system to elucidate the folded states of disease relevant proteins in an AggTag based approach. In addition to future applications toward monitoring the perturbations of proteostasis, we ultimately envision that the combination of this "turn-off" technology and "turn-on" assay can be expanded to enable the high-throughput screening of therapies to influence the cellular proteostasis.

RESULTS AND DISCUSSION

Tunability of Rhodamine Spirocyclization Enables a Resolution of AgHalo Folded States *In Vitro*

In order to establish a chemical trend, we began with the design and synthesis of a small library of rhodaminwse derived probes functionalized with chloroalkane linkers for conjugation to AgHalo (Figure 2a). The library was designed from the basal tetramethylrhodamine probe (**P1**) with the intent of tuning the equilibrium constant for the spirocyclization process toward favoring the closed, nonexcitable form. This was achieved structurally by two strategies. First, we aimed to increase the nucleophilicity of the attacking moiety in the form of an electron deficient lactam moiety (**P2**).[28] Second, the electrophilicity of the xanthene was increased by substitution of the 10′ oxygen for a gem-dimethyl silicon group, yielding the Si-rhodamine derivative, **P3**.[29] Combining the two strategies, we synthesized the hydroxymethyl Si-rhodamine probe, **P4**.[25] Prior to application in the AgHalo assay described above, we elected to analyze the polarity sensitivity of the spirocyclization process by quantifying the fluorescence emission intensity as a function of the dielectric constant in mixtures of 1,4-dioxane and water (Figure 2b). The polarity dependence of the equilibrium constant for spirocyclization (ε_{50}) was calculated as the half-maximum of a sigmodial fit of the titration curves. Relative to the basal TMR probe (**P1**), both strategies for tuning the polarity sensitivity effectively increased the value of ε_{50} (from 7.92−8.05 for **P1** to 49.33−49.82 and 40.08−40.50 for **P2** and **P3**, respectively). Comparison of the hydroxymethyl Si-rhodamine derivative (**P4**, ε_{50} = 29.64−30.06) to the carboxylic acid derivatives is complicated by the drastic differential in pK_a of the zwitterionic species.

The rhodamine derivatives (**P1**−**P4**) were employed in the AgHalo *in vitro* aggregation assay (Figure 3a) in order to characterize the sensitivity of each toward protein folded states (Figure 3). Given the low ε_{50} value, **P1** revealed a modest 1.7-fold decrease in emission intensity upon aggregation of AgHalo (Figure 3b). This sensitivity is nearly doubled with the application of **P2** and **P3**, wherein an approximate 4-fold difference is observed in both cases (Figure 3c and d). Combining the strategies of increasing both the nucleophilicity of the attacking group and the electrophilicity of the xanthene ring with **P4** yielded a 12.7-fold decrease in fluorescence emission upon the aggregation of AgHalo (Figure 3e). Given the correlation between the polarity sensitivity of the spirocyclization equilibrium and fluorogenicity of rhodamine derived probes upon binding to the protein of interest, we elected to visualize the relationship between sensitivity to AgHalo aggregation and fluorogenicity upon binding (Figure 3f).[27] Fluorogenicity was quantified as the fold-change in absorbance upon binding of the probe to AgHalo. The data reveal a linear, positive correlation between the two properties, indicating that the spirocyclization process governs the difference in emission properties, between the protein's folded and aggregate states. Taken together, these data show that the tunable properties of rhodamine derivates enable the detection of protein folded states, with **P4** meeting the necessary fold-change to achieve adequate resolution in downstream applications in living cells.

Human superoxide dismutase 1 (SOD1) is a Cu/Zn binding enzyme responsible for the elimination of deleterious reactive

https://doi.org/10.1021/acsbiomedchemau.3c00012
ACS Bio Med Chem Au 2024, 4, 111−118

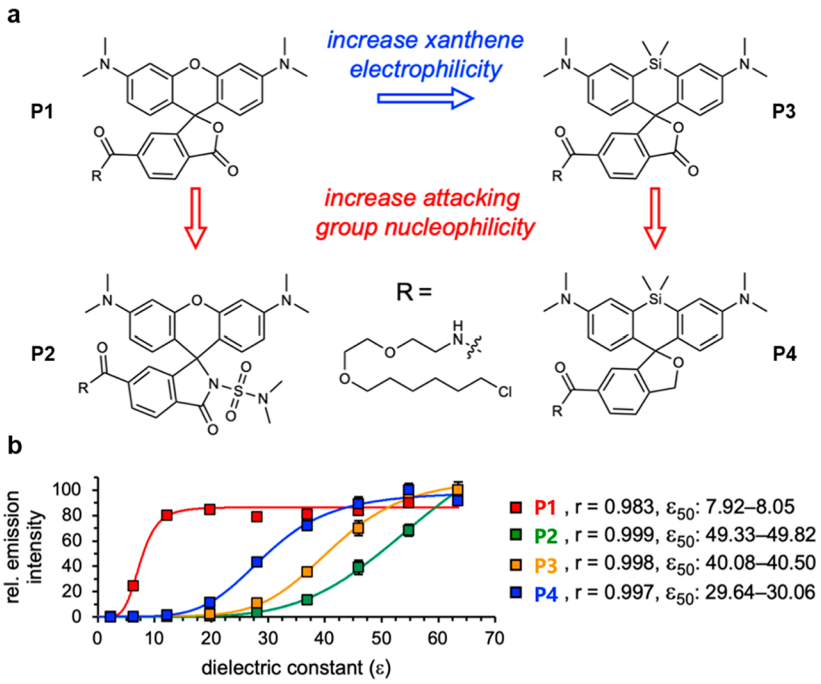

Figure 2. Design of polarity sensitive rhodamine-based probes for the development of a "turn-off" fluorescence-based assay. (a) Structures of rhodamine-based probes for HaloTag **P1**−**P4**. (b) Polarity sensitivity characterization of **P1**−**P4** in water: dioxane gradients (0−80% water v/v). Corresponding *r* values and ε_{50} ranges are presented for the obtained sigmoidal curve fits (shown as smooth lines). (Standard error, $n = 3$.)

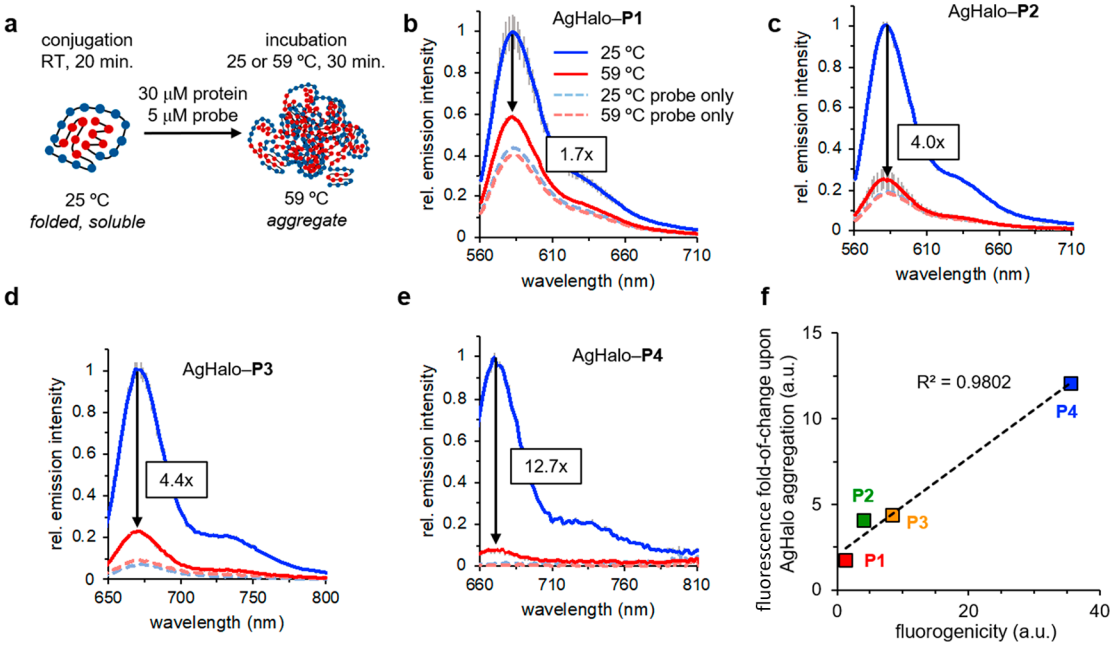

Figure 3. Fluorogenic rhodamines enable sufficient fold-change to monitor protein folded states in the AgHalo *in vitro* characterization assay. (a) Design of AgHalo *in vitro* characterization assay. Thermally induced aggregation of an (b) AgHalo−**P1** (Excitation: 540 nm), (c) AgHalo−**P2** (Excitation: 540 nm), (d) AgHalo−**P3** (Excitation: 630 nm), and (e) AgHalo−**P4** (Excitation: 640 nm) conjugate. (f) Correlation between aggregation-induced emission intensity fold-change and fluorogenicity (absorbance conjugate/probe only in DPBS buffer, 5 μM probe). (Standard error, $n = 3$.)

oxygen species. SOD1 mutants are associated with familial amyotrophic lateral sclerosis, including the aggregation prone SOD1(A4V) and SOD1(V31A) variants.[30−33] With the utility of **P4** established in the AgHalo system, we next aimed to ascertain whether the probe could be applied to such a disease relevant protein using an AggTag based approach. **P4** was conjugated to purified SOD1(A4V)-HaloTag fusion and subjected to thermally induced aggregation at 59 °C (Figure 4a). The results show a near 24-fold reduction in fluorescence emission intensity relative to the soluble conjugate (25 °C). In a dual-probe assay employing both **P4** and **AgHalo 550** (Figure 4c), epifluorescence microscopy was used to directly validate that aggregation was indeed responsible for the difference in the emission intensity (Figure 4b). The images show diffuse

https://doi.org/10.1021/acsbiomedchemau.3c00012
ACS Bio Med Chem Au 2024, 4, 111−118

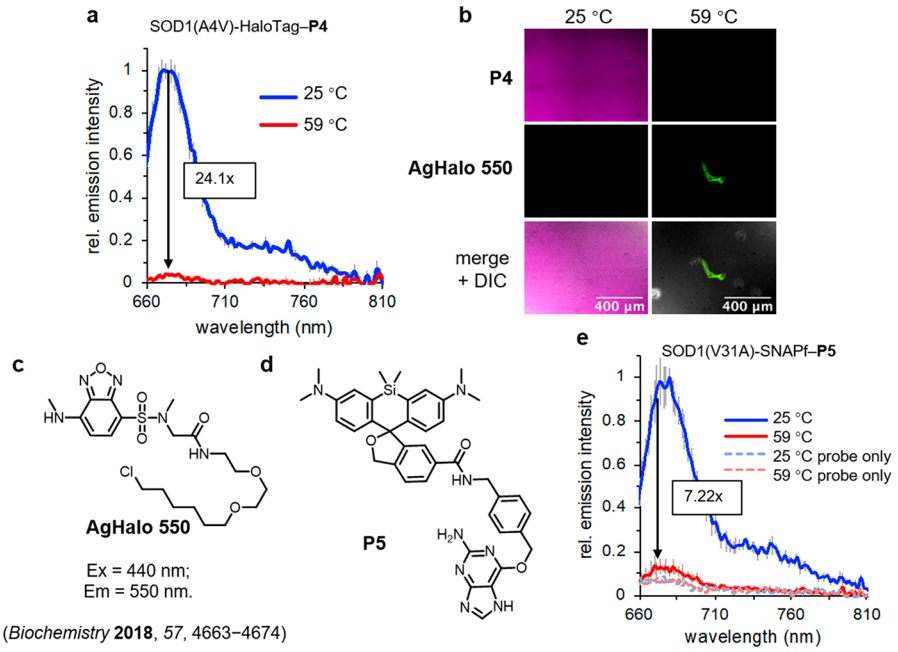

Figure 4. Application of the hydroxymethyl Si-rhodamine fluorophore toward an AggTag approach. (a) Thermally induced aggregation of SOD1(A4V)-HaloTag (25 μM) conjugated to **P4** (5 μM) in DPBS buffer containing 80 mM EDTA. Excitation: 640 nm. (b) Epifluorescence microscopic images of thermally induced aggregation of SOD1(A4V)-HaloTag (25 μM) labeled with **P4** (5 μM) and **AgHalo 550** (5 μM). (c) Structure of probe **AgHalo 550**. (d) Structure of the SNAP-tag probe **P5**. (e) Thermally induced aggregation of SOD1(V31A)-SNAPf (25 μM) conjugated to **P5** (5 μM) in Tris·HCl buffer (pH = 7.5) containing 80 mM EDTA and 2 mM DTT. Excitation: 640 nm (standard error, n = 3).

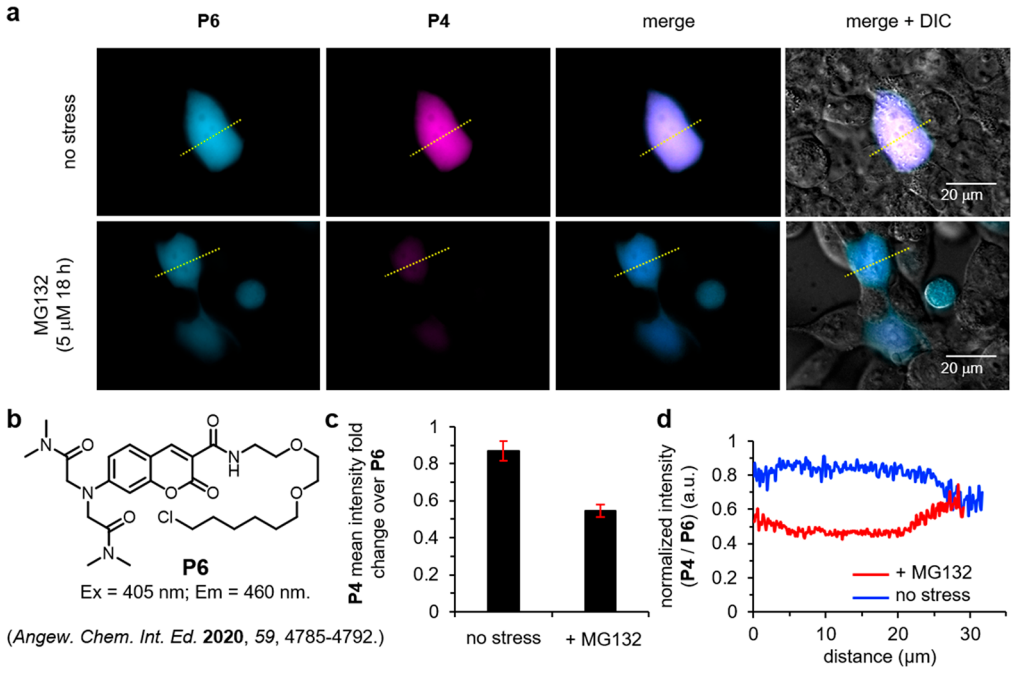

Figure 5. Hydroxymethyl Si-rhodamine probe **P4** in conjugation with AgHalo enables visualization of the perturbation of cellular proteostasis. (a) Epifluorescence microscopic images of HEK293T transiently expressing AgHalo. (b) Structure of probe **P6**. (c) Quantification of mean pixel fluorescence intensity relative to **P6** from three independent images (standard error, n = 3). (d) Quantification of intensity profiles of **P4** relative to **P6** corresponding to the yellow dashed lines in panel (a).

fluorescence for **P4** in the soluble control (25 °C), but no fluorescence upon thermally induced aggregation at 59 °C. In contrast, **AgHalo 550** emission is not observed in the soluble state, while the protein aggregates emit bright green fluorescence.

Multicolor imaging has been used in an AggTag based approach to visualize the effects of proteome stress on two independent proteins *in vivo*.[14,20] Orthogonal labeling mandated dual transfection of plasmids each encoding one of the proteins of interest (POIs) fused to either HaloTag or SNAP-tag. In order to ascertain whether the hydroxylmethyl Si-rhodamine

https://doi.org/10.1021/acsbiomedchemau.3c00012
ACS Bio Med Chem Au 2024, 4, 111−118

probe could be applied in this type of assay, we synthesized **P5** functionalized with an O^6-benzylguanine substrate for SNAP-tag (Figure 4d).[34−39] Conjugation of **P5** to SOD1(V31A)-SNAPf followed by thermal induction of aggregation revealed a 7.2-fold reduction in the emission intensity relative to the soluble control (Figure 4e). These data indicate that the hydrophobic microenvironment of protein aggregates formed by tagged SOD1 mutants is sufficient to enable a reduction in the emission intensity of both **P4** and **P5**, although **P5** remains less effective than **P4**. In order to improve upon the resolution of the SNAP-tag probe, it is necessary to increase the fluorogenicity upon binding to the POI. This may be achieved through variation of the linker structure to yield more favorable interactions with the aqueous solvent and the polar protein surface. Ultimately, these results support the plausibility of the use of fluorogenic rhodamines in an AggTag assay in living cells to screen for conditions that induce misfolding and aggregation of disease relevant proteins.

Visualization of the Perturbation of Cellular Proteostasis

Given the utility of **P4** in the differentiation between protein folded states *in vitro*, we aimed to determine whether a difference in the fluorescence intensity could be observed between live populations of healthy and stressed cells. HEK293T cells transiently expressing AgHalo were treated with equimolar amounts of the hydroxymethyl Si-rhodamine probe, **P4**, and **P6** (Figure 5b) in order to control for differences in expression level. **P6** is a blue-emission fluorescent probe, that was used as an "always-on" probe in cellular imaging.[40−42] In a previous work,[43] we showed that the polarity-sensitivity of coumarins is mostly eliminated for **P6** due to the β-carbonyl groups. As a control probe, its fluorescence emission should change minimally with polarity; and thus, **P6** is an appropriate control probe in this work. Both **P4** and **P6** exhibited minimal cytotoxicity to HEK293T cells under the concentration of 0.5 μM[13,18,43] (Figure S1). In a pulse-chase assay, the unbound labeling probes were removed via washing prior to treatment with a blocking reagent, 6-chlorohexanol. To induce proteostatic stress, cells were treated with the proteasome inhibitor, MG132, while the unstressed population was treated with only the DMSO vehicle. Epifluorescence cellular microscopy was used to visualize differences in emission intensity of **P4** relative to the **P6** expression level control (Figure 5a). Only AgHalo expressing cells can be stained by probes P4 and P6 due to the biorthogonality of the AggTag method used in our experiments. Cells without fluorescence signals are live cells, which cannot express AgHalo protein or label with probes. The results indicate that emission from **P4** decreases by 1.6-fold relative to **P6** upon MG132 induced experiments. Cells without fluorescence signals are live cells which cannot express AgHalo protein or label with probes. The results indicate that emission from **P4** decreases by 1.6-fold relative to **P6** upon MG132 induced proteome stress. These results were quantified by mean intensity fold-change of three independent images for each condition as well as cross-section intensity profiles (Figure 5c and d). Ultimately, the imaging data further support the utility of **P4** in the visualization of the cellular perturbation of proteome stress.

CONCLUSION

This work demonstrates the plausibility of this methodology to visualize the perturbation of cellular proteostasis using fluorogenic derivatives of rhodamine-based dyes. In this context, the proposed assay provides several advantages over current methods to do so, including a real-time pulse-chase fluorescence readout. Further, the nature of this assay is nonmechanistic specific, meaning the discovery of a therapy is possible without aiming for a particular target or system. In this manner, the technology combing the "turn-off" assay with a "turn-on" fluorescence assay may be a potential method used for high-throughput drug discovery methods or as a reliable assay to evaluate the safety of potential therapeutic candidates prior to their application in clinical research.

Provided the utility of fluorogenic rhodamines in single molecule localization techniques and in no-wash labeling strategies, the chemical space of these structures has been well explored in literature. Utilizing these existing chemical strategies, the opportunity for further improvement of the probe's sensitivity remains. Moreover, the development of sensitized fluorogenic rhodamines with blue-shifted excitation and emission properties can be used to enable multicolor AggTag based systems to monitor the folded states and multiple protein targets simultaneously. Such an approach would broaden the application and utility of the presented proteostasis therapy screening assay.

EXPERIMENTAL SECTION

Purification of AgHalo Protein

AgHalo protein was purified according to a previously established procedure. *E. coli* BL21-(DE3*) competent cells harboring an ampicillin-resistant pBAD vector encoding for σ32-I54N were transformed with a kanamycin-resistant pET29b vector encoding for HaloTag(K73T)−His. Five mL of Luria broth (LB) medium was inoculated with a single colony of the transformed cells and shaken rigorously. The inoculation medium was diluted (1:106) with LB medium to a final volume of 50 mL. The diluted starter culture was grown overnight while shaking at 37 °C to OD_{600} ∼ 1.25. Two growth cultures were initiated by addition of 15 mL starter to 1.5 L of ampicillin and kanamycin containing LB medium. Cultures were grown to OD_{600} ∼ 0.30 over 2.5 h while shaking at 37 °C. σ32-I54N expression was induced with the addition of 0.2% (w/v) L-arabinose to each culture. The temperature was reduced to 30 °C, and the cultures were grown until the OD_{600} ∼ 0.7. Expression of HaloTag(K73T)−His was induced by the addition of isopropyl β-D-1-thiogalactopyranoside (0.5 mM final concentration), the incubation temperature was reduced to 18 °C, and expression was allowed to proceed overnight while shaking. Cells were harvested by centrifugation, and the pellets were resuspended in DPBS buffer (10 mL per liter of culture) containing 1 mM phenylmethylsulfonyl fluoride protease inhibitor. Resuspension was transferred to an aluminum beaker and chilled on ice. Cells were lysed by sonication (180 × 2 s pulses at 60% amplitude with 8 s pauses between each pulse) while maintaining a temperature of 4 °C. The lysate was centrifuged (16,000*g*) for 60 min at 4 °C, and the supernatant was isolated and loaded onto a precharged 6 mL NiNTA column. Unbound protein was eluted with 12 column volumes of 50 mM Tris·HCl buffer (pH 7.5) containing 100 mM NaCl. Bound protein was eluted with linear gradient addition (0−100%) of 50 mM Tris·HCl buffer (pH 7.5) containing 100 mM NaCl and 500 mM imidazole over 8 column volumes. The eluted proteins were concentrated and purified by size-exclusion using a 120 mL HiPrepTM 16/60 SephacrylTM S200HR column, eluting with 132 mL of 50 mM Tris·HCl buffer (pH 7.5) containing 100 mM NaCl. The protein containing fractions were identified by SDS-PAGE analysis concentrated. No significant impurities were identified and purity of the HaloTag target protein was estimated to be >95% based on the SDS-PAGE analysis.

In Vitro Aggregation Assays

Purified AgHalo (30 μM) and the corresponding probe (5 μM) were incubated at room temperature in DPBS buffer for 20 min to allow for conjugation. The probe-protein conjugate was incubated at 25 or 59 °C for 30 min. 50 μL sample aliquots were transferred to a 96-well black

https://doi.org/10.1021/acsbiomedchemau.3c00012
ACS Bio Med Chem Au 2024, 4, 111−118

polystyrene plate (Costar), and emission spectra were recorded using a Tecan M1000Pro fluorescence plate reader with the indicated excitation wavelength.

Purified SOD1(A4V)-HaloTag or SOD1(V31A)-SNAPf (25 μM) and the corresponding **P4** or **P5** (5 μM) were incubated at room temperature in tris·HCl buffer (50 mM tris·HCl, 100 mM NaCl, pH 7.5) for 20 min. Buffers were spiked with 2 mM DTT for assays utilizing SNAP-tag. EDTA (80 mM) was added, and the solution was incubated at 25 or 59 °C for 30 min. 50 μL sample aliquots were transferred to a 96-well black polystyrene plate (Costar), and emission spectra were recorded using a Tecan M1000Pro fluorescence plate reader with excitation at 640 nm.

In Vitro Aggregate Imaging

Purified SOD1(A4V)-HaloTag (25 μM), **P4** (5 μM), and **AgHalo 550** (5 μM) were incubated at room temperature in tris·HCl buffer (50 mM tris·HCl, 100 mM NaCl, pH 7.5) for 20 min. EDTA (80 mM) was added, and the solution was incubated at 25 or 59 °C for 30 min. The solution was transferred to a glass slide equipped with a rubber spacer and topped with a glass coverslip. Imaging was completed using a Zeiss Axio Observer.Z1/7 and an EC Plan-Neofluar 10*x*/0.30 Ph 1 objective. **P4** fluorescence was obtained using a 630 nm LED light source, collecting emission through a band-pass filter from 659 to 759 nm. **AgHalo 550** fluorescence was obtained using a 430 nm LED light source, collecting emission through a band-pass filter from 546 to 564 nm. Nonfluorescent images were obtained using differential interference contrast (DIC) microscopy.

Cellular Imaging: AgHalo Expression, MG132 Stress

HEK293T cells suspended in 2 mL of Dulbecco's Modified Eagle's Medium (DMEM) were seeded at 10% confluency in a MatTek poly-D-lysine coated, 35 mm imaging dish fitted with a No. 1.5 glass bottom and incubated at 37 °C (5% CO_2) for 24 h. One mL of media was removed from each imaging chamber and replaced with fresh DMEM containing 2× concentrations of **P4** and **P6** (final conc. 0.5 μM). Transient transfection of AgHalo was achieved by direct addition of 200 μL of a premixed solution containing 2 μg of plasmid encoding AgHalo in a pHTN vector and 4 μL of X-tremeGENETM 9 transfection in Opti-MEM to each culture. Transfection and labeling were allowed to proceed for 24 h while incubating at 37 °C (5% CO_2). Adding probes at the time of transfection would ensure ensure the AgHalo protein could be efficiently labeled during their translation. If the probes were added after AgHalo aggregates, the lack of three-dimensional structure would not allow labeling. Unbound probe was washed out by replacing 2 mL of probe containing media from each culture with fresh DMEM and incubating at 37 °C (5% CO_2) for 30 min. The washout media was replaced with fresh DMEM containing a 6-chlorohexanol blocking reagent for HaloTag (1 μM) and MG132 proteasome inhibitor (5 μM) or the DMSO vehicle only. Cells were stressed for 18 h while incubating at 37 °C (5% CO_2). Imaging was completed using a Zeiss Axio Observer.Z1/7 and a Plan-Apochromat 63×/1.40 Oil DIC M27 objective. **P4** fluorescence was obtained using a 630 nm LED light source, collecting emission through a band-pass filter from 659 to 759 nm. **P6** fluorescence was obtained using a 385 nm LED light source, collecting emission through a band-pass filter from 420 to 470 nm. Nonfluorescent images were obtained using differential interference contrast (DIC) microscopy.

■ ASSOCIATED CONTENT

Supporting Information

The Supporting Information is available free of charge at https://pubs.acs.org/doi/10.1021/acsbiomedchemau.3c00012.

Synthetic experimentals and NMR spectra for compounds (PDF)

Accession Codes

AgHalo from *Rhodococcus rhodochrous* (Uniport entry P0A3G2) and superoxide dismutase 1 from *Homo sapiens* (Uniport entry P0014).

■ AUTHOR INFORMATION

Corresponding Authors

Yu Liu − *Dalian Institute of Chemical Physics, Chinese Academy of Sciences, Dalian, Liaoning 116023, China;* orcid.org/0000-0002-0779-1488; Email: liuyu@dicp.ac.cn

Xin Zhang − *Department of Chemistry, School of Science and Research Center for Industries of the Future, Westlake University, Hangzhou 310030 Zhejiang Province, China; Institute of Natural Sciences, Westlake Institute for Advanced Study, Westlake Laboratory of Life Sciences and Biomedicine, Westlake University, Hangzhou 310024 Zhejiang Province, China;* orcid.org/0000-0001-6686-1645; Email: zhangxin@westlake.edu.cn

Authors

Conner Hoelzel − *Department of Chemistry, The Pennsylvania State University, University Park, Pennsylvania 16802, United States*

Yulong Bai − *Dalian Institute of Chemical Physics, Chinese Academy of Sciences, Dalian, Liaoning 116023, China; Department of Chemistry, School of Science and Research Center for Industries of the Future, Westlake University, Hangzhou 310030 Zhejiang Province, China; Institute of Natural Sciences, Westlake Institute for Advanced Study, Westlake Laboratory of Life Sciences and Biomedicine, Westlake University, Hangzhou 310024 Zhejiang Province, China*

Mengdie Wang − *Dalian Institute of Chemical Physics, Chinese Academy of Sciences, Dalian, Liaoning 116023, China*

Complete contact information is available at: https://pubs.acs.org/10.1021/acsbiomedchemau.3c00012

Author Contributions

⊥C.H. and Y.B. contributed equally to this work. CRediT: **Conner Hoelzel** conceptualization (lead), data curation (equal), formal analysis (equal), investigation (equal), methodology (equal), project administration (equal), resources (equal), supervision (equal), validation (equal), visualization (equal), writing-original draft (equal); **Yulong Bai** visualization (equal), writing-original draft (equal); resources (equal); **Mengdie Wang** resources (equal); **Yu Liu** investigation (equal), methodology (equal), resources(equal), supervision (equal), funding acquisition(equal),; **Xin Zhang** conceptualization (equal), data curation (equal), formal analysis (lead), investigation (lead), methodology (lead), project administration (equal), resources (equal), funding acquisition(equal), supervision (equal), validation (lead), visualization (equal), writing-original draft (equal), writing-review and editing (lead);

Notes

The authors declare no competing financial interest.

■ ACKNOWLEDGMENTS

This work is supported by the Burroughs Welcome Fund Career Award at the Scientific Interface 1013904 (X.Z.), Sloan Research Fellowship FG-2018-10958 (X.Z.), and PEW Biomedical Scholars Program 00033066 (X.Z.). We thank the

Research Center for Industries of the Future (RCIF) at Westlake University for supporting this work.

ABBREVIATIONS

TMR, tetramethylrhodamine; SOD1, Human superoxide dismutase 1; POI, protein of interset

REFERENCES

(1) Bolognesi, B.; Kumita, J. R.; Barros, T. P.; Esbjorner, E. K.; Luheshi, L. M.; Crowther, D. C.; Wilson, M. R.; Dobson, C. M.; Favrin, G.; Yerbury, J. J. ANS binding reveals common features of cytotoxic amyloid species. *Acs Chem. Biol.* **2010**, *5* (8), 735−40.

(2) Abedini, A.; Plesner, A.; Cao, P.; Ridgway, Z.; Zhang, J.; Tu, L. H.; Middleton, C. T.; Chao, B.; Sartori, D. J.; Meng, F.; Wang, H.; Wong, A. G.; Zanni, M. T.; Verchere, C. B.; Raleigh, D. P.; Schmidt, A. M. Time-resolved studies define the nature of toxic IAPP intermediates, providing insight for anti-amyloidosis therapeutics. *Elife* **2016**, *5*, e12977.

(3) Radwan, M.; Wood, R. J.; Sui, X. J.; Hatters, D. M. When Proteostasis Goes Bad: Protein Aggregation in the Cell. *Iubmb Life* **2017**, *69* (2), 49−54.

(4) Chiti, F.; Dobson, C. M. Protein Misfolding, Amyloid Formation, and Human Disease: A Summary of Progress Over the Last Decade. *Annu. Rev. Biochem.* **2017**, *86*, 27−68.

(5) Guo, J. L.; Lee, V. M. Cell-to-cell transmission of pathogenic proteins in neurodegenerative diseases. *Nat. Med.* **2014**, *20* (2), 130−8.

(6) Wang, Y.; Mandelkow, E. Tau in physiology and pathology. *Nat. Rev. Neurosci.* **2016**, *17* (1), 22.

(7) Lin, M. T.; Beal, M. F. Mitochondrial dysfunction and oxidative stress in neurodegenerative diseases. *Nature* **2006**, *443* (7113), 787−95.

(8) Bhat, A. H.; Dar, K. B.; Anees, S.; Zargar, M. A.; Masood, A.; Sofi, M. A.; Ganie, S. A. Oxidative stress, mitochondrial dysfunction and neurodegenerative diseases; a mechanistic insight. *Biomed. Pharmacother.* **2015**, *74*, 101−10.

(9) Hetz, C.; Saxena, S. ER stress and the unfolded protein response in neurodegeneration. *Nat. Rev. Neurol.* **2017**, *13* (8), 477−491.

(10) Li, F.; Lan, X.; Liang, X.-J. Intracellular aggregations of biological elements: From simple to complex. *Aggregate* **2021**, *2* (3), No. e27.

(11) Sabouri, S.; Liu, M. J.; Zhang, S. X.; Yao, B. C.; Soleimaninejad, H.; Baxter, A. A.; Armendariz-Vidales, G.; Subedi, P.; Duan, C.; Lou, X. D.; Hogan, C. F.; Heras, B.; Poon, I. K. H.; Hong, Y. N. Construction of a Highly Sensitive Thiol-Reactive AIEgen-Peptide Conjugate for Monitoring Protein Unfolding and Aggregation in Cells. *Adv. Healthc. Mater.* **2021**, *10* (24), 2101300.

(12) Owyong, T. C.; Hong, Y. Emerging fluorescence tools for the study of proteostasis in cells. *Curr. Opin. Chem. Biol.* **2022**, *67*, No. 102116.

(13) Shen, B.; Jung, K. H.; Ye, S.; Hoelzel, C. A.; Wolstenholme, C. H.; Huang, H.; Liu, Y.; Zhang, X. A dual-functional BODIPY-based molecular rotor probe reveals different viscosity of protein aggregates in live cells. *Aggregate* **2023**, e301.

(14) Liu, Y.; Fares, M.; Dunham, N. P.; Gao, Z.; Miao, K.; Jiang, X.; Bollinger, S. S.; Boal, A. K.; Zhang, X. AgHalo: A Facile Fluorogenic Sensor to Detect Drug-Induced Proteome Stress. *Angew. Chem., Int. Ed.* **2017**, *56* (30), 8672−8676.

(15) Wolstenholme, C. H.; Hu, H.; Ye, S.; Funk, B. E.; Jain, D.; Hsiung, C. H.; Ning, G.; Liu, Y.; Li, X.; Zhang, X. AggFluor: Fluorogenic Toolbox Enables Direct Visualization of the Multi-Step Protein Aggregation Process in Live Cells. *J. Am. Chem. Soc.* **2020**, *142* (41), 17515−17523.

(16) Fares, M.; Li, Y.; Liu, Y.; Miao, K.; Gao, Z.; Zhai, Y.; Zhang, X. A Molecular Rotor-Based Halo-Tag Ligand Enables a Fluorogenic Proteome Stress Sensor to Detect Protein Misfolding in Mildly Stressed Proteome. *Bioconjugate Chem.* **2018**, *29* (1), 215−224.

(17) Liu, Y.; Wolstenholme, C. H.; Carter, G. C.; Liu, H. B.; Hu, H.; Grainger, L. S.; Miao, K.; Fares, M.; Hoelzel, C. A.; Yennawar, H. P.; Ning, G.; Du, M. Y.; Bai, L.; Li, X. S.; Zhang, X. Modulation of Fluorescent Protein Chromophores To Detect Protein Aggregation with Turn-On Fluorescence. *J. Am. Chem. Soc.* **2018**, *140* (24), 7381−7384.

(18) Liu, Y.; Miao, K.; Li, Y. H.; Fares, M.; Chen, S. Y.; Zhang, X. A HaloTag-Based Multicolor Fluorogenic Sensor Visualizes and Quantifies Proteome Stress in Live Cells Using Solvatochromic and Molecular Rotor-Based Fluorophores. *Biochemistry* **2018**, *57* (31), 4663−4674.

(19) Fares, M.; Zhang, X. Quantification of Cellular Proteostasis in Live Cells by Fluorogenic Assay Using the AgHalo Sensor. *Curr. Protoc. Chem. Biol.* **2019**, *11* (1), No. e58.

(20) Jung, K. H.; Kim, S. F.; Liu, Y.; Zhang, X. A Fluorogenic AggTag Method Based on Halo- and SNAP-Tags to Simultaneously Detect Aggregation of Two Proteins in Live Cells. *ChemBioChem.* **2019**, *20* (8), 1078−1087.

(21) Reichardt, C. Solvatochromic Dyes as Solvent Polarity Indicators. *Chem. Rev.* **1994**, *94* (8), 2319−2358.

(22) Haidekker, M. A.; Theodorakis, E. A. Molecular rotors–fluorescent biosensors for viscosity and flow. *Org. Biomol. Chem.* **2007**, *5* (11), 1669−78.

(23) Haidekker, M. A.; Theodorakis, E. A. Environment-sensitive behavior of fluorescent molecular rotors. *J. Biol. Eng.* **2010**, *4*, 11.

(24) Lukinavicius, G.; Umezawa, K.; Olivier, N.; Honigmann, A.; Yang, G. Y.; Plass, T.; Mueller, V.; Reymond, L.; Correa, I. R.; Luo, Z. G.; Schultz, C.; Lemke, E. A.; Heppenstall, P.; Eggeling, C.; Manley, S.; Johnsson, K. A near-infrared fluorophore for live-cell super-resolution microscopy of cellular proteins. *Nat. Chem.* **2013**, *5* (2), 132−139.

(25) Uno, S. N.; Kamiya, M.; Yoshihara, T.; Sugawara, K.; Okabe, K.; Tarhan, M. C.; Fujita, H.; Funatsu, T.; Okada, Y.; Tobita, S.; Urano, Y. A spontaneously blinking fluorophore based on intramolecular spirocyclization for live-cell super-resolution imaging. *Nat. Chem.* **2014**, *6* (8), 681−689.

(26) Lukinavicius, G.; Reymond, L.; Umezawa, K.; Sallin, O.; D'Este, E.; Gottfert, F.; Ta, H.; Hell, S. W.; Urano, Y.; Johnsson, K. Fluorogenic Probes for Multicolor Imaging in Living Cells. *J. Am. Chem. Soc.* **2016**, *138* (30), 9365−9368.

(27) Zheng, Q.; Ayala, A. X.; Chung, I.; Weigel, A. V.; Ranjan, A.; Falco, N.; Grimm, J. B.; Tkachuk, A. N.; Wu, C.; Lippincott-Schwartz, J.; Singer, R. H.; Lavis, L. D. Rational Design of Fluorogenic and Spontaneously Blinking Labels for Super-Resolution Imaging. *ACS Cent. Sci.* **2019**, *5* (9), 1602−1613.

(28) Wang, L.; Tran, M.; D'Este, E.; Roberti, J.; Koch, B.; Xue, L.; Johnsson, K. A general strategy to develop cell permeable and fluorogenic probes for multicolour nanoscopy. *Nat. Chem.* **2020**, *12* (2), 165.

(29) Koide, Y.; Urano, Y.; Hanaoka, K.; Terai, T.; Nagano, T. Evolution of Group 14 Rhodamines as Platforms for Near-Infrared Fluorescence Probes Utilizing Photoinduced Electron Transfer. *Acs Chem. Biol.* **2011**, *6* (6), 600−608.

(30) Saeed, M.; Yang, Y.; Deng, H. X.; Hung, W. Y.; Siddique, N.; Dellefave, L.; Gellera, C.; Andersen, P. M.; Siddique, T. Age and founder effect of SOD1 A4V mutation causing ALS. *Neurology* **2009**, *72* (19), 1634−9.

(31) Araki, T.; Nagano, S.; Tateno, M.; Kaido, M.; Ogata, K.; Arima, K. Misfolded SOD1 forms high-density molecular complexes with synaptic molecules in mutant SOD1-linked familial amyotrophic lateral sclerosis cases. *J. Neurol. Sci.* **2012**, *314* (1−2), 92−6.

(32) Luchinat, E.; Barbieri, L.; Rubino, J. T.; Kozyreva, T.; Cantini, F.; Banci, L. In-cell NMR reveals potential precursor of toxic species from SOD1 fALS mutants. *Nat. Commun.* **2014**, *5*, 5502.

(33) Paez-Colasante, X.; Figueroa-Romero, C.; Sakowski, S. A.; Goutman, S. A.; Feldman, E. L. Amyotrophic lateral sclerosis: mechanisms and therapeutics in the epigenomic era. *Nat. Rev. Neurol.* **2015**, *11* (5), 266−79.

(34) Juillerat, A.; Gronemeyer, T.; Keppler, A.; Gendreizig, S.; Pick, H.; Vogel, H.; Johnsson, K. Directed evolution of O6-alkylguanine-DNA alkyltransferase for efficient labeling of fusion proteins with small molecules in vivo. *Chem. Biol.* **2003**, *10* (4), 313−7.

https://doi.org/10.1021/acsbiomedchemau.3c00012
ACS Bio Med Chem Au 2024, 4, 111−118

(35) Keppler, A.; Gendreizig, S.; Gronemeyer, T.; Pick, H.; Vogel, H.; Johnsson, K. A general method for the covalent labeling of fusion proteins with small molecules in vivo. *Nat. Biotechnol.* **2003**, *21* (1), 86−9.
(36) Keppler, A.; Pick, H.; Arrivoli, C.; Vogel, H.; Johnsson, K. Labeling of fusion proteins with synthetic fluorophores in live cells. *Proc. Natl. Acad. Sci. U. S. A.* **2004**, *101* (27), 9955−9.
(37) Juillerat, A.; Heinis, C.; Sielaff, I.; Barnikow, J.; Jaccard, H.; Kunz, B.; Terskikh, A.; Johnsson, K. Engineering substrate specificity of O6-alkylguanine-DNA alkyltransferase for specific protein labeling in living cells. *ChemBioChem.* **2005**, *6* (7), 1263−9.
(38) Gronemeyer, T.; Chidley, C.; Juillerat, A.; Heinis, C.; Johnsson, K. Directed evolution of O6-alkylguanine-DNA alkyltransferase for applications in protein labeling. *Protein. Eng. Des. Sel.* **2006**, *19* (7), 309−16.
(39) Mollwitz, B.; Brunk, E.; Schmitt, S.; Pojer, F.; Bannwarth, M.; Schiltz, M.; Rothlisberger, U.; Johnsson, K. Directed evolution of the suicide protein O(6)-alkylguanine-DNA alkyltransferase for increased reactivity results in an alkylated protein with exceptional stability. *Biochemistry* **2012**, *51* (5), 986−94.
(40) Grimm, J. B.; English, B. P.; Chen, J. J.; Slaughter, J. P.; Zhang, Z. J.; Revyakin, A.; Patel, R.; Macklin, J. J.; Normanno, D.; Singer, R. H.; Lionnet, T.; Lavis, L. D. A general method to improve fluorophores for live-cell and single-molecule microscopy. *Nat. Methods* **2015**, *12* (3), 244−250.
(41) Cao, D.; Liu, Z.; Verwilst, P.; Koo, S.; Jangjili, P.; Kim, J. S.; Lin, W. Coumarin-Based Small-Molecule Fluorescent Chemosensors. *Chem. Rev.* **2019**, *119* (18), 10403−10519.
(42) Cheng, Z. M.; Kuru, E.; Sachdeva, A.; Vendrell, M. Fluorescent amino acids as versatile building blocks for chemical biology. *Nat. Rev. Chem.* **2020**, *4* (6), 275−290.
(43) Hoelzel, C. A.; Hu, H.; Wolstenholme, C. H.; Karim, B. A.; Munson, K. T.; Jung, K. H.; Zhang, H.; Liu, Y.; Yennawar, H. P.; Asbury, J. B.; Li, X.; Zhang, X. A General Strategy to Enhance Donor-Acceptor Molecules Using Solvent-Excluding Substituents. *Angew. Chem., Int. Ed.* **2020**, *59* (12), 4785−4792.

https://doi.org/10.1021/acsbiomedchemau.3c00012
ACS Bio Med Chem Au 2024, 4, 111−118